Tuning Optical Properties and Enhancing Solid-State Emission of Poly(thiophene)s by Molecular Control: A Postfunctionalization Approach

Yuning Li,† George Vamvounis, and Steven Holdcroft*

Department of Chemistry, Simon Fraser University, 8888 University Drive, Burnaby, BC V5A 1S6 Canada

Received January 28, 2002; Revised Manuscript Received June 3, 2002

ABSTRACT: Postfunctionalization of poly(3-hexylthiophene) (P3HT) enables the systematic study of electronic and steric effects of various functional groups on the optical and photophysical properties of 3,4-disubstituted poly(thiophene)s. In solution, these 3,4-disubstituted poly(thiophene)s exhibit a lower fluorescence yield (Φ_{fl}) than P3HT. In the solid state, bromo, chloro, and formyl groups increase Φ_{fl}, whereas nitro groups completely quench fluorescence. Phenyl, *p*-tolyl, 2- and 4-methoxyphenyl, 2-thienyl, biphenyl, and 1-naphthyl substituents increase the solid-state fluorescence of P3HT by a factor of 2−3 as a result of steric interactions that force the aromatic substituents perpendicular to the main chain. An extensive enhancement in the solid-state Φ_{fl}, 12 times greater than that of P3HT, is observed for polymers containing *ortho*-alkylphenyl or 2-(3-alkyl)thienyl groups, because of additional steric interactions between methyl or α-methylene hydrogens on the phenyl or thienyl substituents and main-chain thienyl groups. These interactions further increase the planarity of the polymer backbone and lead to an enlargement of the interplanar distance. Partial substitution of P3HT with *o*-tolyl groups affords polymer films with a solid-state Φ_{fl} of up to 22%.

Introduction

Polymer-based light-emitting devices (LEDs) have received much attention in recent years as potential components for large-area displays.[1] A large proportion of research in this field has been directed toward poly(*para*-phenylenevinylene) (PPV) and poly(fluorene) derivatives because of their relatively high emission efficiencies compared to those of other conjugated polymers.[1c] However, the environmental stability of PPVs can be problematic because their labile vinylene groups are easily oxidized, and a limitation of poly(fluorene)s is their narrow range of emission wavelengths, which is restricted to the blue. Consequently, other conjugated polymers with high quantum efficiencies, tunable emission colors, and good stabilities are of interest for the development of polymer LED-based displays.

Poly(thiophene)s have generally been viewed as unsuitable materials for use as emission layers in LEDs because of their relatively low quantum yields.[1c,2] The fluorescence efficiency (Φ_{fl}) of poly(3-alkylthiophene)s is ∼40% in solution but <2% in the solid state. Nonradiative decay via strong interchain interactions[1c] and intersystem crossing caused by the heavy-atom effect of sulfur[3] are believed to be responsible for the low value of Φ_{fl} in films. To weaken interchain interactions and increase Φ_{fl}, poly(thiophene)s have been diluted in inert polymer matrixes.[4,5] However, phase separation results in re-aggregation of poly(thiophene)s, and the quantum efficiency decreases over time. In another approach, Inganäs et al. reported a polythiophene derivative, poly(2,5-dioctylphenylthiophene), that shows a high Φ_{fl} (24%) in the solid state.[6] The two octyl groups on the phenyl substituent are believed to force the phenyl group perpendicular to the main-chain plane to form molecular "bumpers" that prevent close contact between polymer chains. Their results imply that the quantum efficiency of poly(thiophene)s in the solid state can be enhanced by appropriate molecular engineering. In addition, poly(thiophene)s are considered thermally and chemically stable relative to many other conjugated polymers, and red to blue emission colors can be obtained by changing the substituents on the thiophene rings.[1e,7] Accordingly, poly(thiophene)s can still be considered promising as light-emitting layers if deficiencies in their quantum efficiencies can be adequately addressed.

Scheme 1

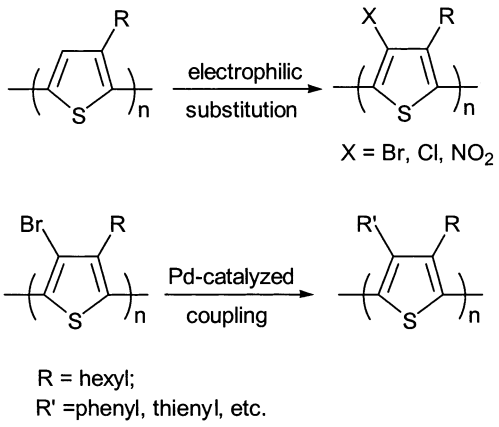

Recently, we reported postfunctionalization of commercially available poly(3-hexylthiophene) with a variety of functional groups (Schemes 1 and 2).[8,9] This methodology facilitates structural engineering of poly(thiophene) derivatives and provides an opportunity for the systematic investigation of the influence of different substituents on the photophysical properties of poly-

* To whom correspondence should be addressed.
† Present address: Institute for Chemical Process and Environmental Technology, National Research Council of Canada, Ottawa, ON, K1A 0R6 Canada.

10.1021/ma020140o CCC: $22.00
Published on Web 08/01/2002

Scheme 2

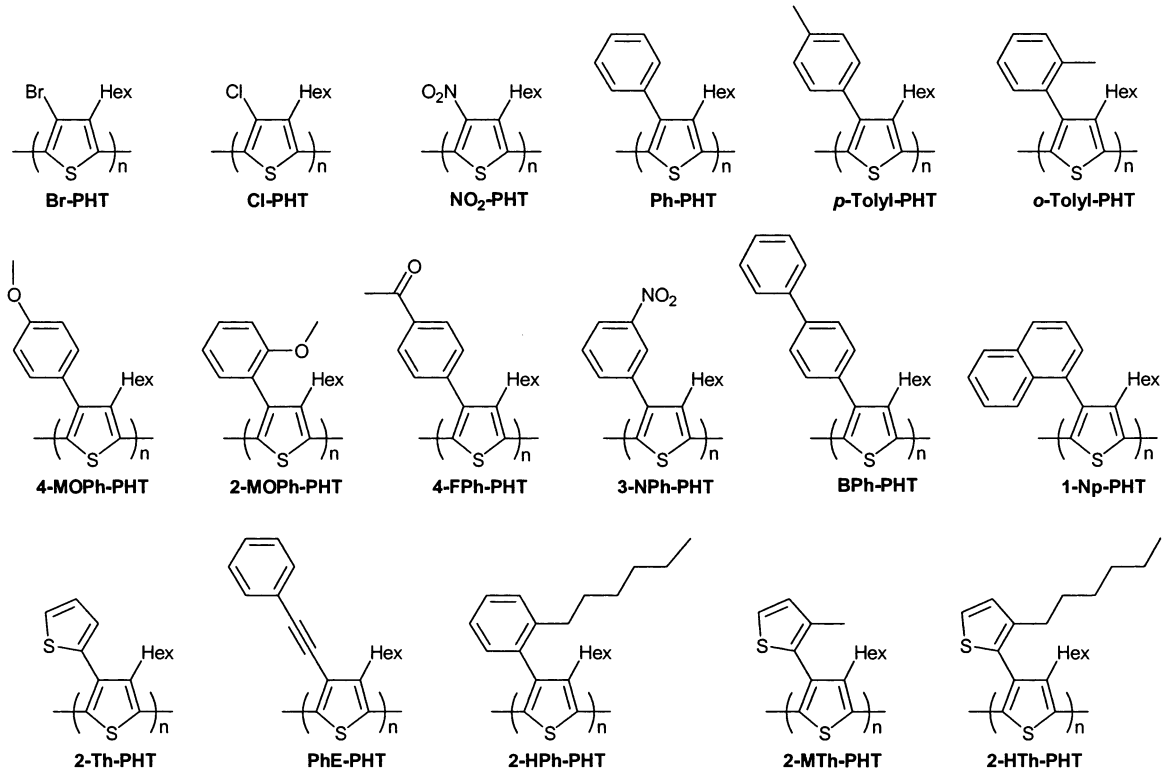

(thiophene)s without the tedium of having to synthesize and polymerize a variety of different monomers and also without the concern that the degree of polymerization of the various polymers might vary significantly. In this paper, we report on the role of various substituents on the optical and photophysical properties of 3,4-disubstituted poly(thiophene)s.

Results and Discussion

The syntheses of Br-PHT, Cl-PHT, and NO_2-PHT by electrophilic substitution of regioregular poly(3-hexylthiophene) (P3HT) were reported previously.[8] The brominated polymer (Br-PHT) was transformed by Pd-catalyzed Suzuki or Stille coupling to yield a spectrum of 3,4-disubstituted polymers containing various functional groups (Scheme 2).[9] The complete substitution of bromo groups was confirmed by NMR spectroscopy and elemental analysis.

As shown in Table 1, the optical spectrum of Br-PHT is blue-shifted (λ_{max}, 339 nm) with respect to that of P3HT, indicating an increased degree twisting of the polymer backbone. A decrease in Φ_{fl} to 4% in solution (40.1% for P3HT) is observed because of the shortened conjugation length, a reduction in the rigidity of the polymer, and possibly the heavy-atom effect[10] of bromine. The solid-state Φ_{fl} of Br-PHT is not appreciably improved (Φ_{fl}, 1.8%) compared to that of P3HT (Φ_{fl}, 1.6%), despite its twisted structure, an observation explained in terms of the heavy-atom effect. On the other hand, the chlorinated product Cl-PHT shows a smaller blue shift in absorption λ_{max}, compared to Br-PHT, and a much higher Φ_{fl} (solution, 12%; solid state, 5.1%). The weaker heavy-atom effect of chlorine and a relief in steric congestion due to the smaller size of chloro group might both contribute to the above result. More dramatic still, the introduction of a nitro group at the 4 position of the thiophene ring results in the virtual absence of fluorescence emission, indicating that the nitro group is a strong quencher of excitation.

Table 1. Photophysical Properties of 3,4-Disubstituted Poly(thiophene)s

	solution			films		
polymer	$\lambda_{max,abs}$ (nm)	$\lambda_{max,em}$ (nm)	Φ_{fl} (%)	$\lambda_{max,abs}$ (nm)	$\lambda_{max,em}$ (nm)	Φ_{fl} (%)
P3HT	442	571	40.1	550	660, 730	1.6
Br-PHT	339	504	4.0	344	520	1.8
Cl-PHT	357	516	12.0	365	527	5.1
NO_2-PHT	338	556	0.3			
Ph-PHT	363	528	7.9	369	553	3.2
p-Tolyl-PHT	364	529	8.0	368	550	3.3
o-Tolyl-PHT	400	545	20.8	410	556	19.4
4-MOPh-PHT	367	531	8.2	375	538	3.0
2-MOPh-PHT	367	535	9.7	376	545	4.4
4-FPh-PHT	350	540	3.4	360	540	2.5
3-NPh-PHT	354	nd[a]	~0	356	nd[a]	~0
BPh-PHT	275	360	1.1			
	360	531	5.8	367	538	3.3
1-Np-PHT	370	540	8.8	378	542	2.6
2-Th-PHT	370	540	8.8	378	542	5.0
PhE-PHT	403	567	7.0	415	602	4.0
2-HPh-PHT	413	555	25.1	422	583	19.6
2-MTh-PHT	401	544	12.8	405	558	9.0
2-HTh-PHT	404	544	14.2	410	555	13.9

[a] Not determined.

Replacing the bromo group in Br-PHT with phenyl to produce Ph-PHT causes the λ_{max} of absorption to red shift from 339 to 363 nm for polymers in solution. Φ_{fl} increases from 4 to 7.9% in solution and from 1.8 to 3.2% in the solid state (Table 1). The attachment of electron-donating 4-methyl and 4-methoxy groups to the phenyl ring, forming *p*-Tolyl-PHT and 4-MOPh-PHT, respectively, has little influence either on λ_{max} for absorption and emission or on Φ_{fl} when compared to the corresponding values for Ph-PHT. This indicates that the phenyl group is electronically isolated from the π-conjugated polythiophene backbone. BPh-PHT, which con-

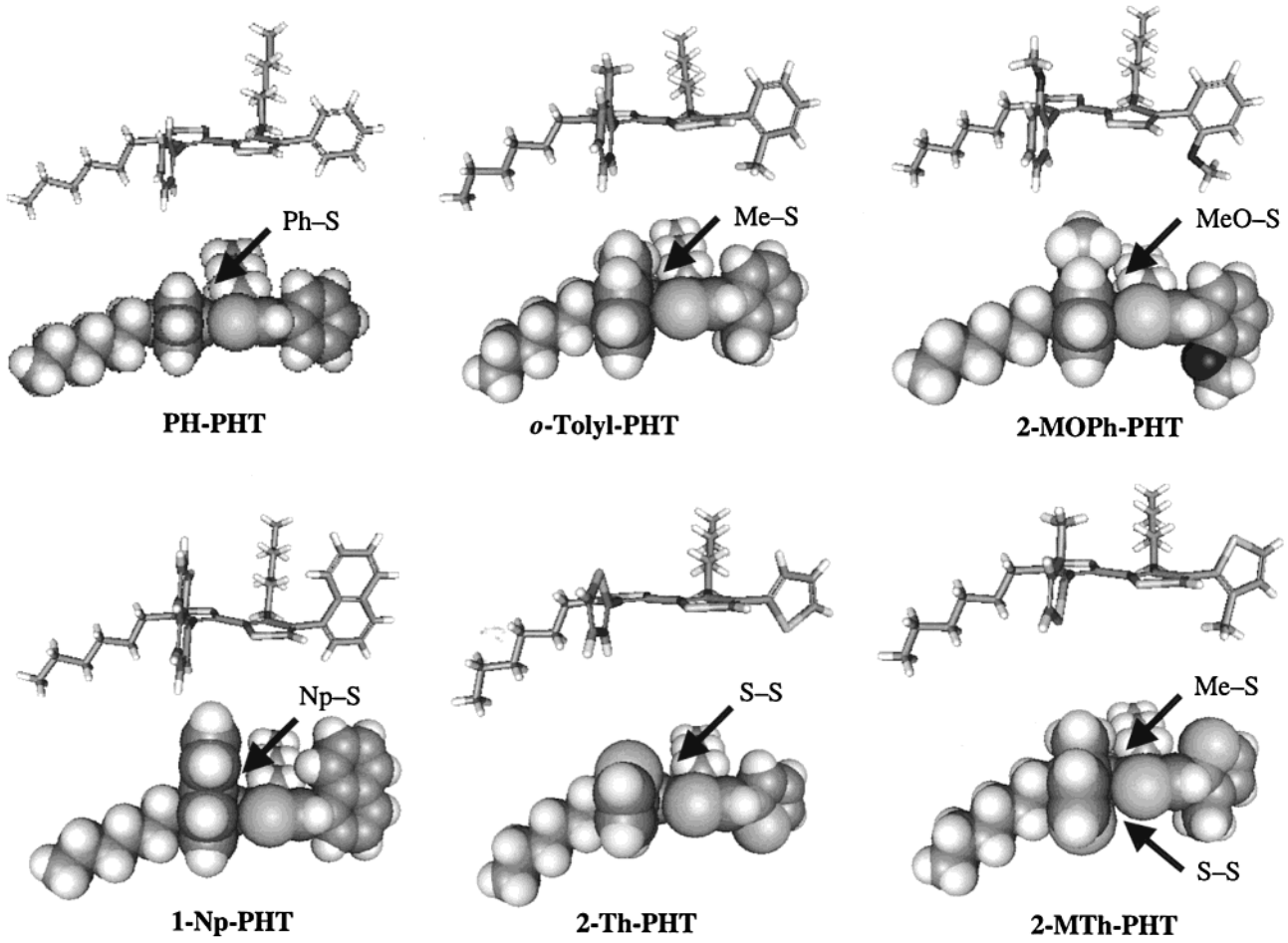

Figure 1. Illustrative molecular models of dyad units for various polymers. The arrows highlight the presence or absence of steric interactions of substituents with the neighboring sulfur atom.

tains biphenyl substituents, exhibits two absorption peaks: one at 275 nm and the other at 360 nm. The former coincides precisely with that of the biphenyl group, whereas the latter is due to the backbone π system. Furthermore, the absorption and emission profiles originating from excitation of the polymer backbone are similar to those of Ph-PHT. Like the phenyl, *p*-tolyl, and 4-methoxyphenyl substituents, the biphenyl groups in BPh-PHT appear, to a first approximation, to act as isolated chromophores. This can only be possible if the chromophores lie perpendicular to the thiophene ring. Introduction of the electron-withdrawing 4-formyl group on the phenyl ring (4-FPh-PHT) causes a slight blue shift in absorption λ_{max} and a decrease in solution Φ_{fl} (3.4%). Substitution of Br with 3-nitrophenyl (3-NPh-PHT) causes a slight blue shift in absorption λ_{max} relative to that of Ph-PHT, but it also results in the absence of fluorescence, even though the nitro group at the meta position is virtually electronically isolated from the polymer backbone. The 2-thienyl-substituted polymer (2-Th-PHT) exhibits absorption and emission maxima in a range similar to those of the phenyl derivatives. Another derivative, the phenylethylenyl-substituted polymer (PhE-PHT), however, displays large red shifts in absorption λ_{max} (403 nm, solution; 410 nm, solid state) as a result of the linear ethylenyl group alleviating steric repulsion. This facilitates planarity of the polymer backbone, which, together with the electron-donating effect of the phenylethylenyl groups, narrows the band gap. The observed electronic effect of the ethylenyl group, more pronounced than the effects of other substituents, is due to efficient overlapping of linear sp orbitals with the main-chain π system. Φ_{fl} of this polymer (7%, solution; 4%, solid state) is not appreciably different from that of Ph-PHT. A significant deviation from the above trends is observed for the *o*-tolyl-substituted polymer (*o*-Tolyl-PHT). This polymer exhibits a large red shift in λ_{max} and unusually high solution and solid-state values of Φ_{fl} (20.8 and 19.4%, respectively) compared to Ph-PHT. The solid-state Φ_{fl} is an order of magnitude higher than those of P3HT (1.6%) and Br-PHT (1.8%). We attribute this to the steric effect of the *o*-tolyl substituent. As illustrated in the structural model shown in Figure 1, the steric interaction of the *o*-tolyl group with the hexyl substituent on the juxtaposed thienyl ring, and more importantly with the neighboring sulfur atom, reinforces the orthogonality of the phenyl ring with respect to the thienyl ring. The *o*-methyl group of *o*-Tolyl-PHT can come into such close proximity to the sulfur atom that it restricts rotation or twisting of the interannular bond between the two thienyl rings. This conformation forces the polymer backbone to become planar and promotes a red shift in λ_{max}. In addition, the methyl group, together with a near-perpendicular phenyl ring, functions as a molecular spacer that enlarges the distance between stacks of polymer chains and, hence, increases the solid-state value of Φ_{fl}. Figure 1 also illustrates that a similar interaction between the phenyl group alone in Ph-PHT and the adjacent thienyl sulfur is absent. Thus, twisting of the main chain is impeded to a lesser extent in Ph-PHT than it is in *o*-Tolyl-PHT. Thus, a shorter wave-

length of absorption and a lower solid-state Φ_{fl} value is observed for Ph-PHT. This explanation is supported by the fact that *p*-Tolyl-PHT, which contains a methyl group in the para position, i.e., far removed from the possibility of a methyl−thienyl sulfur interaction, exhibits properties akin to those of Ph-PHT and not those of *o*-Tolyl-PHT.

2-MOPh-PHT, 4-MOPh-PHT, and 1-Np-PHT, which contain *o*-methoxyphenyl, *p*-methoxyphenyl, and 1-naphthyl, respectively, also display optical and luminescence properties that are very similar to those of Ph-PHT even though these substituents are considerably bulkier than a simple phenyl. Although the *o*-methoxy group is not too dissimilar to *o*-tolyl, Figure 1 illustrates that the oxygen atom is too small, and the methyl group too far removed from the polymer backbone, to limit rotation of the backbone via interaction with the main-chain sulfur atom. In the case of 1-Np-PHT, Figure 1 illustrates that the 1-naphthyl group is too planar to interact with the adjacent sulfur atom. The above observations indicate that a subtle variation in the size or shape of the substituents greatly impacts the backbone conformation and ultimately its optical and photophysical properties. In the case of *o*-Tolyl-PHT, the methyl hydrogens on the *o*-tolyl group are in such a position to limit rotation of the polymer backbone.

To test this hypothesis, several structural analogues of *o*-Tolyl-PHT, namely, 2-HPh-PHT, 2-MTh-PHT, and 2-HTh-PHT, were designed and synthesized using Br-PHT as the base polymer (see Scheme 2). A common structural feature of 2-HPh-PHT, 2-MTh-PHT, and 2-HTh-PHT is the alkyl substituent on the phenyl or thienyl side group having a point of attachment that is juxtaposed to the polymer chain. Solution and film spectra of 2-HPh-PHT are slightly red-shifted by 12−13 nm (λ_{max}, 413 and 422 nm, respectively) with respect to those of *o*-Tolyl-PHT, and Φ_{fl} increases to 25.1% in solution, indicating that the longer alkyl side chain on the phenyl group further increases the planarity and rigidity of the backbone. The solid-state Φ_{fl} (19.6%) is similar to *o*-Tolyl-PHT. A similar red shift in optical absorption is observed for 2-(3-methyl)thienyl and 2-(3-hexyl)thienyl groups. For example, λ_{max} values in solution are 401 nm for 2-MTh-PHT and 404 nm for 2-HTh-PHT compared to 370 nm for the 2-thienyl-substituted polymer 2-Th-PHT. Φ_{fl} values for 2-MTh-PHT and 2-HTh-PHT are 12.8 and 14.2% in solution and 9.0 and 13.9% in the solid state, respectively. These values are much higher than those for 2-Th-PHT (8.8%, solution; 5.0%, solid state). Similarly to the case of *o*-Tolyl-PHT vs Ph-PHT, the methyl hydrogens on the 2-methylthienyl group of 2-MTh-PHT can sterically interfere with the sulfur on the adjacent main-chain thienyl group thus limiting rotation about the main-chain interannular bond (see Figure 1). A similar argument can be made for 2-HTh-PHT and 2-HPh-PHT, where the hexyl α-methylene hydrogens of the 2-hexylthienyl and 2-hexylphenyl substituents might interact with the neighboring main-chain sulfur atom.

Although *o*-alkylphenyl- and 2-(3-alkyl)thienyl-substituted polymers exhibit red-shifted absorption spectra relative to Ph-PHT or 2-Th-PHT, their effective conjugation lengths, as judged by the absorption and emission spectra, are nevertheless lower than that of the parent polymer P3HT. Because fluorescence quantum efficiency is perceived to increase with conjugation length,[11] it was considered that partial substitution of P3HT would allow for a more conjugated structure, providing a means to increase Φ_{fl} and, at the same time, tune emission wavelengths. Partial substitution of P3HT was achieved by partial bromination of P3HT followed by the appropriate Suzuki coupling. As shown in Table 2, a series of partially brominated P3HT polymers (0−100% bromination) was synthesized. The absorption λ_{max} values of the polymer films varied between 550 nm (0% bromination, P3HT) and 344 nm (100% bromination, Br-PHT). The solution Φ_{fl} values decreased from 40.1 to 4% as the degree of substitution increased from 0 to 100%. In contrast, the solid-state Φ_{fl} showed no clear trends except that substituted polymers generally exhibit higher values.

Substitution of the bromo groups in the brominated polymers by *o*-tolyl groups yields the corresponding partially substituted *o*-Tolyl-PHT polymers. The λ_{max} of absorption decreases with increasing degree of substitution from 442 to 400 nm in solution and from 550 to 410 nm in the solid state, but the decrease is less pronounced than that for the corresponding brominated derivatives. Φ_{fl} of the corresponding polymer solutions generally decreases with increasing degree of substitution, but the solid-state Φ_{fl} increases, reaching a maximum value of 22.3% for *o*-Tolyl-PHT89. In addition, the

Table 2. Photophysical Properties of Partially Substituted P3HT

	solution			films		
polymer	$\lambda_{max,abs}$ (nm)	$\lambda_{max,em}$ (nm)	Φ_{fl} (%)	$\lambda_{max,abs}$ (nm)	$\lambda_{max,em}$ (nm)	Φ_{fl} (%)
Br-PHT0[a]	442	571	40.1	550	660, 730	1.6
10	439	570	36.7	535	710	1.8
20	425	570	32.3	515	718	3.2
38	408	561	27.6	433	656	1.8
50	388	556	20.9	405	620	5.0
67	367	548	11.9	378	590	3.6
75	359	535	9.4	370	571	4.0
89	352	520	6.3	359	559	4.4
100[b]	339	504	4.0	344	520	1.8
o-Tolyl-PHT0[a]	442	571	40.1	550	660, 730	1.6
10	444	570	35.7	537	710	2.5
20	442	570	34.2	528	708	3.1
38	437	569	28.2	492	700	4.4
50	432	566	24.2	460	640	12.8
67	430	566	31.0	462	638	13.2
75	420	563	30.2	437	610	20.5
89	418	561	27.8	432	593	22.3
100[c]	400	545	20.8	410	556	19.4

[a] P3HT in Table 1. [b] Br-PHT in Table 1. [c] *o*-Tolyl-PHT in Table 1.

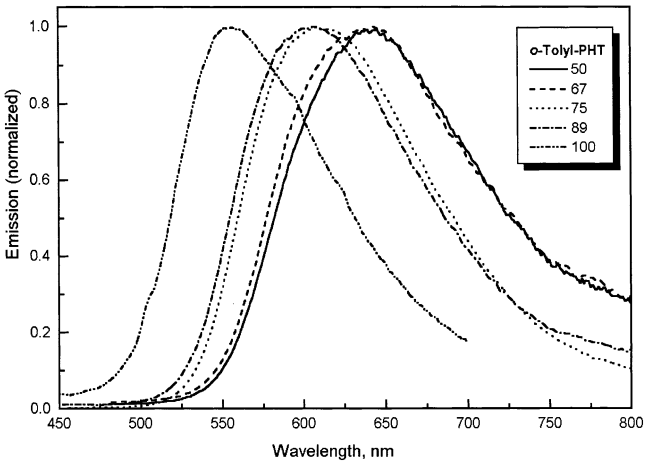

Figure 2. Emission spectra of *o*-tolyl-substituted P3HTs.

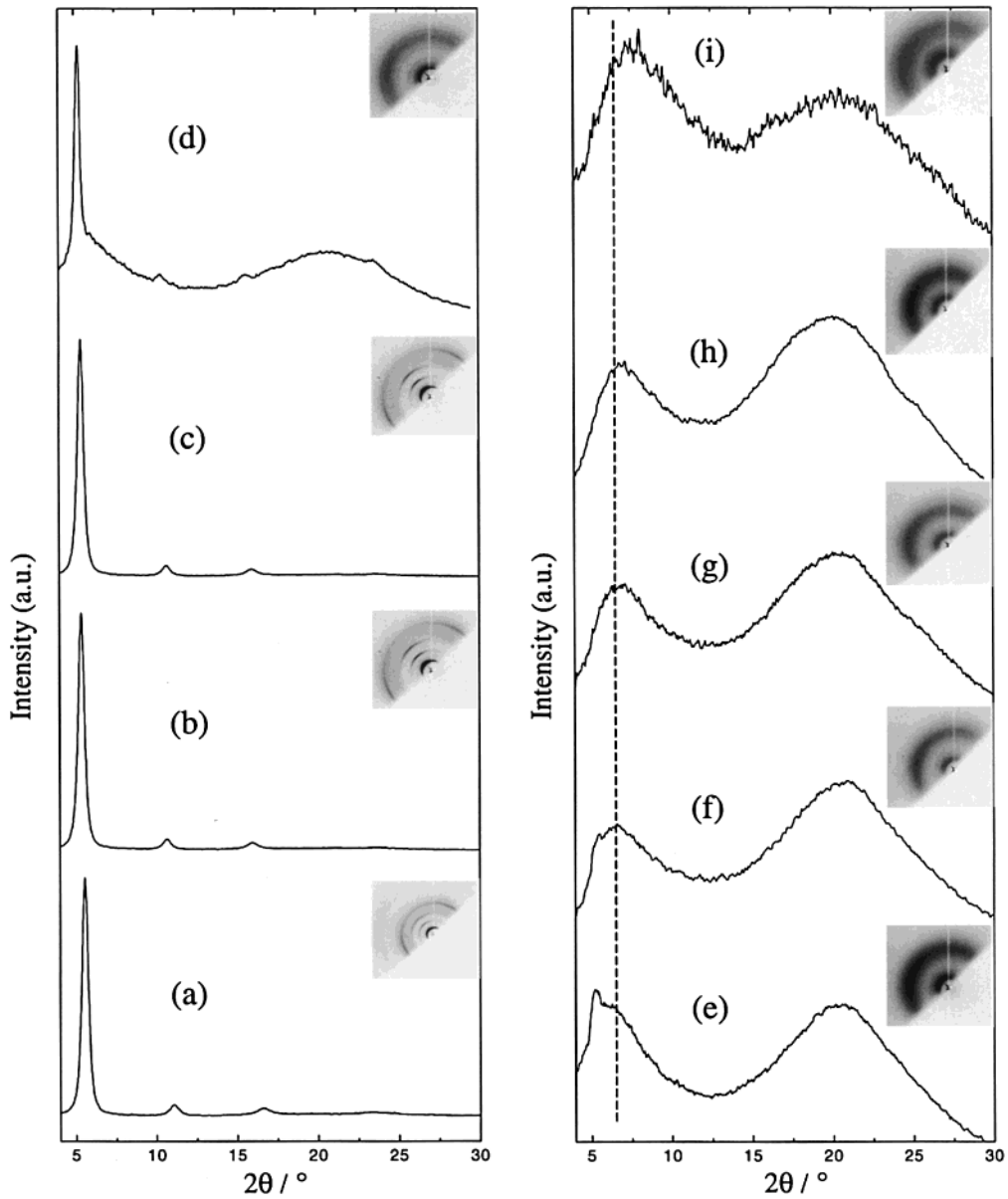

Figure 3. X-ray diffraction patterns of *o*-tolyl-substituted P3HTs: (a) 0, (b) 10, (c) 20, (d) 38, (e) 50, (f) 67, (g) 75, (h) 89, and (i) 100% substitution.

emission wavelengths of polymers are generally red-shifted compared to those of the corresponding Br-substituted polymers. Emission spectra of polymer films having a degree of substitution between 50 and 100% are shown in Figure 2. The emission wavelengths range from 556 to 640 nm.

XRD patterns of various *o*-Tolyl-PHT films are shown in Figure 3. The XRD pattern of P3HT (Figure 3a) exhibits typical diffraction peaks corresponding to lamellae formation (*a* axis, *d* spacing of 16.1 Å).[12,13] The anisotropic nature of the pattern (see inset) and the absence of a peak originating from π stacking (*b* axis) indicates that the chains are orientated with their *a* axis perpendicular to the plane of the substrate. This is also observed for *o*-Tolyl-PHT polymers containing 10 and 20% substitution, as evidenced by strong first-order reflections at $2\theta = 5.35°$ and 5.19°, indicative of 16.5- and 17.0-Å lamellar spacings, respectively. These *a*-axis values are larger than the original *d* spacing corresponding to P3HT, as illustrated in Figure 4, indicating that the *o*-tolyl group interferes with interdigitation of the hexyl side chains.[12c,14] The XRD pattern of *o*-Tolyl-PHT38 also provides evidence that the *o*-tolyl groups disrupts semicrystallinity. First, a broad amorphous peak is observed superimposed on the first-order reflection at 5.19°; and second, a broad amorphous peak corresponding to intermolecular $\pi-\pi$ stacking emerges at $2\theta = 20.8°$. The isotropic nature of the XRD pattern, as can be inferred from the inset of Figure 3d, illustrates that a transition occurs from an ordered polymer with its *a* axis perpendicular to the substrate to one that exhibits no preferential surface ordering. For *o*-Tolyl-PHT50, the peak at $2\theta = 5.25°$, which represents a *d* spacing of 16.8 Å, is much weaker, and two broad peaks at $2\theta = 6.0°$ and 20.4°, which correspond to the calculated *d* spacings of 14.7 and 4.3 Å, respectively, become pronounced. As the degree of substitution is further increased from 50 to 100%, the XRD patterns become weaker, and the position of the second amorphous diffraction/scattering halo at ~20° remains unchanged in its position, whereas the first broad peak shifts incrementally from 6.0° (*d* spacing, 14.7 Å) to 7.6° (*d* spacing, 11.7 Å) to reflect changes in short-range packing of polymer chains. The increasing amorphous

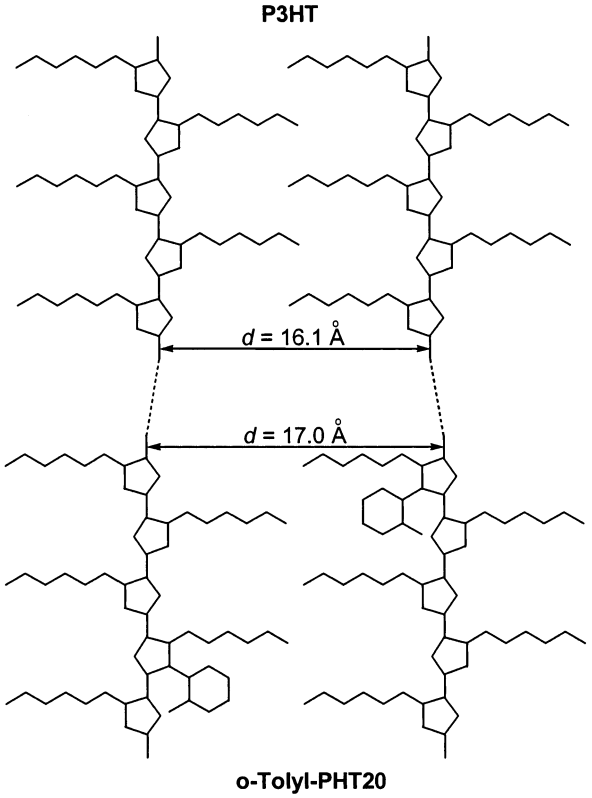

Figure 4. Influence of substitution on the *a*-axis *d* spacing of *o*-tolyl-substituted P3HTs.

nature of polymers with increasing degree of substitution implies that $\pi-\pi$ interactions are progressively suppressed.

Conclusion

Postfunctionalization of poly(3-hexylthiophene) provides an opportunity for the systematic study of the influence of substituents on the photophysical properties of 3,4-disubstituted poly(thiophene)s that exhibit the same degree of polymerization. Substitution with phenyl, *p*-tolyl, 2- and 4-methoxyphenyl, biphenyl, 1-naphthyl, 2-thienyl, and phenylethylenyl groups causes a red shift in the absorption and emission λ_{max} values and a slight increase in the solid-state Φ_{fl}. Polymers containing *o*-tolyl, *o*-hexylphenyl, 2-(3-methyl)thienyl, and 2-(3-hexyl)thienyl groups exhibit a significantly higher Φ_{fl} in the solid state (9−22%) compared to P3HT (1.6%) and Br-PHT (1.8%). The methyl hydrogens on the *o*-tolyl groups and the hexyl α-methylene hydrogens on the 2-hexylthienyl and 2-hexylphenyl substituents serve to limit rotation of the backbone and force the phenyl or thienyl group perpendicular to the main-chain π system. Such a conformation not only increases the planarity and rigidity of the polymer backbone but also enlarges the interplanar distance to the point that highly substituted films are amorphous. The suppression of π stacking, together with rigidification of the main chain, leads to a significant enhancement of luminescence yield.

Molecular order/disorder and optical/photophysical properties of polymers were controlled by partial postfunctionalization of P3HT with *o*-tolyl groups. For degrees of substitution ranging from 50 to 100%, the solid-state Φ_{fl} is enhanced to 13−22%, and the emission wavelength can be readily tuned from 556 to 640 nm. The postfunctionalization approach allows for a series of highly luminescent poly(thiophene)s to be prepared from a weakly luminescent parent poly(3-hexylthiophene). Electroluminescence studies of this new class of light emitting materials are in progress.

Experimental Section

Measurements. ^{1}H NMR spectra were obtained in $CDCl_3$ on a 400-MHz Bruker AMX400 spectrometer; the chemical shifts are reported in parts per million (ppm), referenced to $CHCl_3$ (δ 7.26). IR spectra were recorded on a Bomen Michelson MB series spectrophotometer. UV−vis absorption spectra were obtained on a Cary 3E (Varian) spectrophotometer. Fluorescence measurements were carried out on a PTI QuantumMaster model QM-1 spectrometer. THF solutions of polymers with OD = 0.05−0.1 were deoxygenated prior to fluorescence measurements, and the percentage fluorescence quantum yield (≤10% error) was determined against a quinine bisulfate standard (Φ_{fl} = 54.6% in 1.0 N H_2SO_4). Spin-coated polymer films with OD = 0.1−0.2 were protected under an argon flow during fluorescence measurement and the quantum yield (≤30% error) was reported against 9,10-diphenylanthracene in PMMA ($<10^{-3}$ M) (Φ_{fl} = 83%). X-ray diffractometry was performed on a Rigaku D/MAX-RAPID X-ray microdiffraction system using Cu Kα radiation (λ = 1.5418 Å). Polymer films were prepared on silicon wafer or quartz glass substrate by solution casting of polymers in chloroform and were annealed for 15 min at 150 °C prior to measurement. Molecular models of polymer dyad units were prepared using WebLab ViewerLite (Molecular Simulations, Inc.). In these illustrative examples, the polymer backbone was forced to be coplanar, and aromatic substituents were set perpendicular to the backbone.

Materials. Br-PHT, Cl-PHT, NO_2-PHT, Ph-PHT, *p*-Tolyl-PHT, *o*-Tolyl-PHT, 4-MOPh-PHT, 2-MOPh-PHT, 4-FPh-PHT, 3-NPh-PHT, BPh-PHT, 1-Np-PHT, 2-Th-PHT, and PhE-PHT were prepared by postfunctionalization of a regioregular poly(3-hexylthiophene) as reported previously.[8,9] Partially *o*-tolyl-substituted P3HTs were prepared by (i) partial bromination with NBS and (ii) Suzuki coupling of the brominated polymers with *o*-tolylboronic acid, following a procedure similar to the preparation of *o*-Tolyl-PHT.[9]

2-Hexylphenylboronic Acid. To a solution of 1-bromo-2-hexylbenzene[15] (1.46 g, 6 mmol) in ether (15 mL) at −40 °C was added slowly a solution of *n*-BuLi (2.42 mL, 2.5 M in hexane). The mixture was allowed to warm to room temperature while being stirred for 2 h. The mixture was then added to a solution of trimethylborate (1.87 g, 18 mmol) in ether (20 mL) at −60 °C. After the mixture was allowed to warm to room temperature and stirred for 12 h, 2 N HCl (35 mL) was added. The organic layer was separated, and the aqueous layer was extracted with ether (20 mL). The solvent was removed from the combined organic layers, and a white solid was obtained. Column chromatography (silica gel) of the crude product by hexane and then ether gave a white solid (0.85 g, 77%). ^{1}H NMR (*d*-acetone): δ 7.0−7.5 (m, aromatic protons), 2.82 (m, α-methylene), 1.1−1.4 (m), 0.83 (m, CH_3).

2-(3-Methylthienyl)boronic Acid. To a cooled (−60 °C) solution of trimethylborate (5.3 g, 50.7 mmol) in ether (20 mL) was added 2-(3-methylthienyl) magnesium bromide (16.9 mmol in 30 mL of ether) that had been prepared from magnesium and 2-bromo-3-methylthiophene. After the mixture had been stirred for 12 h at room temperature, 2 N HCl (20 mL) was added. A workup procedure similar to that described above gave the title compound as a white solid (1.21 g, 50%). ^{1}H NMR (*d*-acetone): δ 7.49 (d, J = 5.0 Hz, 1H), 6.96 (d, J = 5.0 Hz, 1H), 5.75 (O*H*), 2.45 (s, CH_3).

2-(3-Hexylthienyl)boronic Acid. Similarly, the reaction of 2-(3-methylthienyl) magnesium bromide (20 mmol in 20 mL of ether) with trimethylborate (6.23 g, 60 mmol in 30 mL of ether) gave the title compound as a semisolid (3.65 g, 86%). ^{1}H NMR (*d*-acetone): δ 7.49 (d, J = 4.9 Hz, 1H), 6.97 (d, J = 4.9 Hz, 1H), 5.75 (O*H*), 2.61 (t, J = 7.6 Hz, α-methylene), 1.2−1.5 (m), 0.86 (m, CH_3).

2-HPh-PHT, 2-MTh-PHT, and 2-HTh-PHT were prepared by Suzuki coupling of Br-PHT with 2-hexylphenylboronic acid, 2-(3-methylthienyl)boronic acid, and 2-(3-hexylthienyl)boronic acid, respectively.[9] Data for 2-HPh-PHT follow. ^{1}H NMR ($CDCl_3$): δ 7.20, 6.81, 2.1−2.7 (m, br, α-methylene), 1.90 (CH_3−Th), 1.15 (br), 1.06 (br), 0.810 (*t*, J = 6.5 Hz, CH_3CH_2−); IR (NaCl): 3058, 3019, 2955, 2926, 2856, 1728, 1465, 1377, 1175, 755 cm^{-1}. Data for 2-MTh-PHT follow. ^{1}H NMR ($CDCl_3$): δ 7.22, 6.86, 2.0−2.6 (m, br, α-methylene), 1.2−1.4 (m, br), 0.83 (t, J = 7.9 Hz, CH_3); IR (NaCl): 3062, 2953, 2923, 2856, 1727, 1455, 1378, 1006, 706 cm^{-1}. Data for 2-HTh-PHT follow. ^{1}H NMR ($CDCl_3$): δ 7.0−7.4 (br), 1.8−2.6 (m, br, α-methylene), 1.1−1.4 (m, br), 0.84 (br), 0.78 (br); IR (NaCl): 3065, 2955, 2926, 2869, 2856, 1728, 1459, 1261, 1086, 1021, 804, 723 cm^{-1}.

Acknowledgment. This work was supported by the Natural Sciences and Engineering Research Council of Canada (NSERC). G.V. thanks NSERC and the Xerox Research Centre of Canada for scholarship support.

Supporting Information Available: UV−vis absorption spectra of Br-PHT, Cl-PHT, NO_2-PHT, Ph-PHT, *p*-Tolyl-PHT, *o*-Tolyl-PHT, 4-MOPh-PHT, 2-MOPh-PHT, 4-FPh-PHT, 3-NPh-PHT, BPh-PHT, 1-Np-PHT, 2-Th-PHT, 2-Th-PHT, PhE-PHT, 2-HPh-PHT, 2-MTh-PHT, 2-HTh-PHT, Br-PHT10, Br-PHT20, Br-PHT38, Br-PHT50, Br-PHT67, Br-PHT75, Br-PHT89, *o*-Tolyl-PHT10, *o*-Tolyl-PHT20, *o*-Tolyl-PHT38, *o*-Tolyl-PHT50, *o*-Tolyl-PHT67, *o*-Tolyl-PHT75, and *o*-Tolyl-PHT89 polymer films are provided. This material is available free of charge via the Internet at http://pubs.acs.org.

References and Notes

(1) (a) Burroughes, J. H.; Bradley, D. D. C.; Brown, A. R.; Marks, H. N.; Mackay, K.; Friend, R. H.; Burns, P. L.; Holmes, A. B. *Nature* **1990**, *347*, 539. (b) Gustafsson, G.; Cao, Y.; Treacy, G. M.; Klavetter, F.; Colaneri, N.; Heeger, A. J. *Nature* **1992**, *357*, 447. (c) Samuel, I. D. W.; Rumble, G.; Friend, R. H. In *Primary Photoexcitations in Conjugated Polymers: Molecular Excitation versus Semiconductor Band Model*; Sariciftci, N. S., Ed.; World Scientific Publishing Co.: Singapore, 1997. (d) Kraft, A.; Grimsdale, A. C.; Holmes, A. B. *Angew. Chem., Int. Ed. Engl.* **1998**, *37*, 402. (e) Yu, G.; Wang, J.; McElvain, J.; Heeger, A. J. *Adv. Mater.* **1998**, *10*, 1431.

(2) (a) Xu, B.; Holdcroft, S. *Macromolecules* **1993**, *26*, 4457. (b) Gill, R. E.; Malliaras, G. G.; Wildeman, J.; Hadziioannou, G. *Adv. Mater.* **1994**, *6*, 132. (c) Greenham, N. C.; Samuel, I. D. W.; Hayes, G. R.; Phillips, R. T.; Kessener, Y. A. R. R.; Moratti, S. C.; Holmes, A. B.; Friend, R. H. *Chem. Phys. Lett.* **1995**, *241*, 89. (d) Chen, F.; Mehta, B.; Takiff, L.; McCullough, R. D. *J. Mater. Chem.* **1996**, *6*, 1763.

(3) Saadeh, H.; Goodson, T., III; Yu, L. *Macromolecules* **1997**, *30*, 4608.

(4) Lemmer, U.; Mahrt, R. F.; Wada, Y.; Greiner, A.; Bässler, H.; Göbler, E. O. *Appl. Phys. Lett.* **1993**, *62*, 2827.

(5) Berggren, M.; Bergman, P.; Fagerström, J.; Inganäs, O.; Anderson, M. R.; Weman, H.; Granström, M.; Stafström, S.; Wennerström, O.; Hjertberg, T. *Chem. Phys. Lett.* **1999**, *304*, 84.

(6) Anderson, M. R.; Berggren, M.; Olinga, T.; Hjertberg, T.; Inganäs, O.; Wennerström, O. *Synth. Met.* **1997**, *85*, 1383.

(7) Anderson, M.; Thomas, O.; Mammo, W.; Svensson, M.; Theander, M.; Inganäs, O. *J. Mater. Chem.* **1999**, *9*, 1933.

(8) Li, Y.; Vamvounis, G.; Holdcroft, S. *Macromolecules* **2001**, *34*, 141.

(9) Li, Y.; Vamvounis, G.; Yu, J.; Holdcroft, S. *Macromolecules* **2001**, *34*, 3130.

(10) Saadeh, H.; Goodson, T., III; Yu, L. *Macromolecules* **1997**, *30*, 4608.

(11) (a) Chosrovian, H.; Rentsch, S.; Grebner, D.; Dahm, D. U.; Brickner, E. *Synth. Met.* **1993**, *60*, 23. (b) Herrema, J. K.; van Hutten, P. F.; Gill, R. E.; Wildeman, J.; Wieringa, R. H.; Hadziioannou, G. *Macromolecules* **1995**, *28*, 8102.

(12) (a) Winokur, M. J.; Spiegel, D.; Kim, Y.; Hotta, S.; Heeger, A. J. *Synth. Met.* **1989**, *28*, C419. (b) Leclerc, M.; Diaz, F. M.; Wegner, G. *Makromol. Chem.* **1989**, *190*, 3105. (c) McCullough, R. D.; Tristram-Nagle, S.; Williams, S. P.; Lowe, R. D.; Jayaraman, M. *J. Am. Chem. Soc.* **1993**, *115*, 4910. (d) Chen, T.; Wu, X.; Rieke, R. D. *J. Am. Chem. Soc.* **1995**, *117*, 233.

(13) Prosa, T. J.; Winokur, M. J.; Moulton, J.; Smith, P.; Heeger, A. J. *Macromolecules* **1992**, *25*, 4364.

(14) Prosa, T. J.; Winokur, M. J.; McCullough, R. D. *Macromolecules* **1996**, *29*, 3654.

(15) Bromo-2-hexylbenzene was prepared by cross-coupling of 1,2-dibromobenzene with hexyl magnesium bromide in the presence of $PdCl_2$(dppb) according to the procedure in: Minato, A.; Tamao, K.; Hayashi, T.; Suzuki, K.; Kumada, M. *Tetrahedron Lett.* **1980**, *21*, 845.

MA020140O